Principal component and sensitivity analysis of cirrus clouds using high-resolution IR radiance spectra: simulations and observations

Brian H. Kahn[1](kahn@atmos.ucla.edu), Annmarie Eldering[1,2], Michael Ghil[1,3], Simona Bordoni[1], Amy Braverman[2], Eric J. Fetzer[2], and Helen M. Steele[1,4]

[1] University of California at Los Angeles, Department of Atmospheric Sciences, Los Angeles, CA, USA. [2] Jet Propulsion Laboratory, California Institute of Technology, Pasadena, CA, USA.

[3] Département Terre-Atmosphère-Océan and Laboratoire de Météorologie Dynamique, Ecole Normale Supérieure, Paris, France. [4] California State University at Northridge, Department of Geography, Northridge, CA, USA

Abstract: A set of simulated and observed nadir-oriented high-resolution infrared (IR) emission spectra of synthetic cirrus clouds is analyzed to assess the spectrally dependent variability of radiance from the adjustment of some microphysical and bulk cirrus cloud properties. A Principal Component Analysis (PCA) is applied to the simulated spectra to diagnose the cloud parameters that contribute most to variations in top-of-atmosphere (TOA) radiance. The properties investigated include particle shape, effective radius (r_{eff}), optical depth (τ), cloud height and thickness, vertical temperature ($T(z)$) and water vapor mixing ratio (w) profiles. It is shown that τ (or IWP) variations in simulated cloud cover contribute most to TOA radiance variations. Further, it can be shown that variability of τ and IWP is nearly identical to first order. Cloud height and thickness, as well as variable $T(z)$ can produce some TOA radiance variability. The shape of empirical orthogonal functions (EOFs) in the radiance spectra shows similarities and differences from one physical quantity to another. When several parameters are combined together it is sometimes possible to identify individual EOFs that represent the variability of particular physical quantities. If small particle r_{eff}, τ, and w variations occur simultaneously, the resultant EOFs resemble spectral signatures of EOFs generated from individually varying r_{eff}, τ, and w, with some distortion in the shape of w. Comparisons of simulated EOFs are made to EOFs of Atmospheric Infrared Sounder radiance spectra (Aumann and Pagano 1994). Fields of principal components (PCs) obtained by projecting the EOFs onto AIRS radiance spectra are compared with model forecast fields.

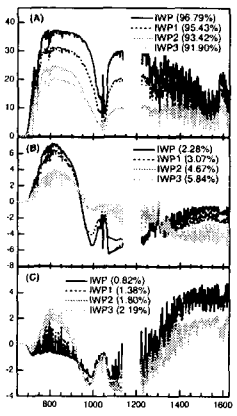

Figure 1. (a) Leading EOF for the variation of IWP, w, and r_{eff} simultaneously using an NCEP AVN model atmosphere of T and w and single-scattering parameters as given in Kahn et al. (2003). Both (b) and (c) are as (a), except for the second and third EOFs, respectively. Explained variance in parentheses. The AVN w profile is scaled by factors of 0.4, 0.6, 0.8, 1.2, 1.4, and 1.6. Increments of IWP include: 10^{-5}, 5×10^{-5}, 10^{-4}, 5×10^{-4}, 10^{-3}, 5×10^{-3}, and 10^{-2} gm^{-2}. Particle sizes are 5.0, 8.0, 11.69, 16.0, 21.0, and 25.3 μm. The run "IWP" includes all IWP values aforementioned; "IWP1" includes all but 10^{-2} gm^{-2}, IWP2, includes all but 5×10^{-3}, and 10^{-2} gm^{-2}, and IWP3 includes all but 10^{-3}, 5×10^{-3}, and 10^{-2} gm^{-2}.

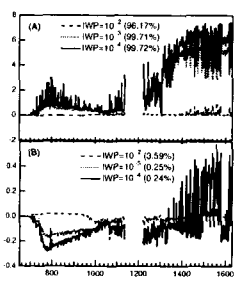

Figure 3. Variation of water vapor for a fixed atmospheric profile (the South American Andes orographic cirrus case), with a cloud fixed at 12-13 km, for an IWP of 10^{-4}, 10^{-3}, and 10^{-2} gm^{-2}, with a $w(z)$ scaled to 0.4, 0.6, 0.8, 1.2, 1.4, and 1.6 of the original values.

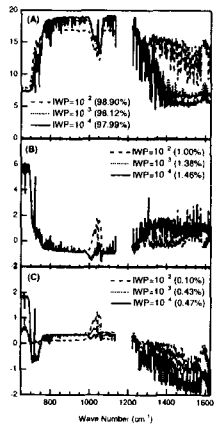

Figure 2. (a) Leading EOF for a variable atmosphere; both $T(z)$ and $w(z)$ are varied, with all other gas profiles fixed. Shown are the EOFs for three IWP values: 10^{-2}, 10^{-3}, and 10^{-4}. Both (b) and (c) are as (a), except for second and third EOFs. Particle size is held at 25.3 μm; the cloud is located between 6-9 km; and cylindrical ice particles with an aspect ratio of 1.0 is used.

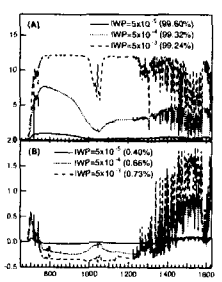

Figure 4. (a) Leading EOF for variation of cloud height. The cloud thickness is fixed to 3 km, and the base (top) is varied from 6-11 (9-14) km. (b) Same as (a) except for second EOF.

Methodology: A set of TOA radiance simulations for cirrus clouds has been produced by the Code for High-resolution Accelerated Radiative Transfer with Scattering (CHARTS), an adding-doubling plane-parallel monochromatic radiative transfer model with multiple scattering (Moncet and Clough 1997), coupled with the Line-By-Line Radiative Transfer Model (LBLRTM). The synthetic cirrus cloud extinction and asymmetry parameter spectra are generated by the *T*-matrix method (Mishchenko et al. 1998), where we have used randomly oriented cylinders and spheroids at an assortment of aspect ratios. The simulations utilize six climatological atmospheres that span typical seasonal and latitudinal ranges of temperature and H_2O vapor. We have adjusted microphysical and bulk properties such as: particle shape, effective radius (r_{eff}), cirrus thickness (Δz_{cld}) and height (z_{cld}), optical depth (τ), and vertical profiles of temperature ($T(z)$) an H_2O vapor mixing ratio (w). All simulations are convolved to 1 cm^{-1} spectral resolution.

Principal Component Analysis (PCA) is used here to investigate the spectral variability of radiance, as well as attribute variability in observed radiances to particular physical parameters by comparing observations with simulations. Simply put, PCA decomposes the variability in a subspace of data (simulated or observed) into a series of basis vectors orthogonal to each other in descending order of importance based on the amount of explained variance in the data by each basis vector. A singular value decomposition (SVD) is applied to a covariance matrix of the simulated or observed radiances perturbed from a mean, which yields eigenvectors and eigenvalues. The eigenvectors are also known as empirical orthogonal functions (EOFs), and each eigenvalue is associated with a particular EOF. The eigenvalue gives information on the relative amount of variance explained by the EOF when compared to the others.

In order to make sense of several EOFs, any given EOF must be attributed to a physical parameter or a unique combination of parameters. PCA on simulations is performed to understand the sort of variability that might be expected with certain physical parameters. PCA can be applied to radiances with only one parameter "tuned", or multiple parameters simultaneously. The "tuning" of single parameters produces EOFs identifiable to that parameter, while applying the same method to multiple parameters is more realistic, because observed radiance spectra are the product of the effects of multiple parameter variations that occur simultaneously. In order to see the relative importance of each EOF on a given synthetic or observed spectrum, we calculate horizontal principal component (PC) fields; a PC is a coefficient that weights the importance of a particular EOF in reproducing an original simulated or observed radiance spectrum. Maps of PCs are produced for particular EOFs and are related to model fields of T_{sfc} and $w(z)$, in addition to brightness temperature (BT). Thus, comparisons between simulated and observed EOFs provide a way to determine if a given EOF (or combination of EOFs) is due to the variability of a particular physical parameter (or several). Comparisons of horizontal PC fields with independent observations or model simulations provides a further check on the linkage between EOFs, PC fields, and the physical fields that cause such variability.

Results: Figures 1-4 present EOFs for the adjustment of several parameters including IWP, r_{eff}, cloud height, $T(z)$, and $w(z)$. Other experiments including aspect ratio, and cloud depth variations with a fixed base or height are not shown here due to space constraints. Figure 1 shows the three leading EOFs for simultaneous variations in r_{eff}, IWP, and w. The two leading EOFs are a combination of IWP and r_{eff} variations. For IWP alone (not shown), the shape of the two leading EOFs resembles very closely the two leading EOFs in Figure 1. However, the effect of particle size is to add some curvature to the 770-1000 cm^{-1} window, as long as IWP is not very large. Thus, it appears that r_{eff} effects can be seen in the presence of IWP changes as long as r_{eff} is smaller than 10s of microns, and IWP is within some nominal low to moderate range.

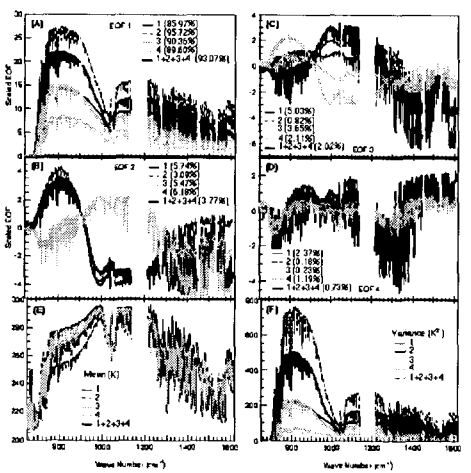

Figure 5. Four leading EOFs for the orographic cirrus scene. (A) Leading EOF for the entire orographic cirrus cloud (1+2+3+4), and for four sub-regions (1, 2, 3, and 4) depicted in Figure 6. Explained variance of the leading EOF in parentheses. (B) - (D): same as (A) except for the second, third, and fourth EOFs. (E) Mean spectra for the entire cloud and sub-regions described in (A). (F) As in (E) except for variance.

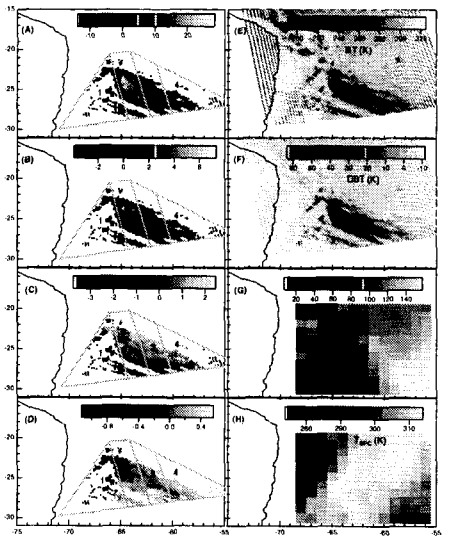

Figure 6. PC maps for the first four leading EOFs for the entire orographic cirrus scene (A)-(D). (F) and (F) are BT at 998 cm^{-1} and ΔBT for 998 - 811 cm^{-1}, respectively. (G) is the column w and (H) is T_{sfc}; both are taken from NCEP AVN model initialized fields at 18Z on October 2nd, 2002. PC fields for sub-scenes 1-4 not shown.

Figure 5 shows the first four EOFs for an orographic cirrus scene in the lee of the South American Andes. The PCs and subsections are shown in Figure 6. EOFs for four subsections, in addition to EOFs for the full scene, are shown along with the mean spectra and variance. The first three EOFs resemble very closely those found in Figure 1. The explained variance of EOF1 in Figure 5 matches best with "IWP1", "IWP2", and "IWP3" in Figure 1; this is an indication that IWP values never get quite as large as the "IWP" case in Figure 1. It should be emphasized that the atmosphere used to model Figure 1 was taken from the NCEP AVN model at the time of the cloud event at 24°S 64°W, with cloud height fixed to 12-13 km.

The four PC fields associated with the four EOFs shown in Figure 5 are found in Figure 6 (a)-(d); these fields are for the entire scene, not for the sub scenes. The boundaries of the sub scenes are denoted by the gray borders. Figure 6e, BT at 998 cm^{-1}, compares very well to PC1. PC2 is not intended to correspond directly with ΔBT: PCs 1 and 2 are a combined effect of IWP and particle size. However, PC3 shows a decent match to the AVN column w field despite the following: (1) the obscuration of the lower level w due to cloud, (2) inaccuracies in the AVN model initialization, and (3) that EOF3 could have contributions from other fields other than $w(z)$. It is also interesting to note that PC4 matches somewhat well with T_{sfc} from the AVN model.

Summary:

- EOFs of simulated and observed high-resolution IR data are compared to match observed EOFs to cloud and atmospheric physical parameters.
- IWP/τ variability explains the dominant one or two EOFs.
- r_{eff} variability distorts shape and changes explained variance of EOF1 and 2: clues to r_{eff} variability if r_{eff} < a few 10s of microns.
- Additional EOFs capture some atmospheric variability, such as $w(z)$ and $T(z)$.
- Some PC fields compare well with independent model data and physical fields inferred from simulated EOFs.
- This case has small r_{eff}, low to moderate IWP, and large horizontal gradients in w and T_{sfc}; thus, most other scenes with less variability other than IWP will be expected to be dominated even more so by a primary EOF caused by IWP.

Acknowledgments: The authors would like to thank S.A. Clough for use of CHARTS and fruitful discussion. B.H. Kahn is funded by a NASA-ESS fellowship. A portion of this work was performed at the Jet Propulsion Laboratory, California Institute of Technology, under contract with NASA.

References:

Aumann, H.H., and R.J. Pagano, 1994: Atmospheric Infrared Sounder on the Earth Observing System. *Opt. Eng.*, **33**, 776-784.

Kahn, B.H., A. Eldering, S.A. Clough, E.J. Fetzer, E. Fishbein, M.R. Gunson, S.-Y. Lee, P.F. Lester, and V.J. Realmuto, 2003: Near micron-sized cirrus cloud particles in high-resolution infrared spectra: An orographic case study. *Geophys. Res. Lett.*, doi:10.1029/2003GL016909.

Kahn, B.H., A. Eldering, M. Ghil, S. Bordoni, and S.A. Clough, 2003: Principal component and sensitivity analysis of cirrus clouds using high-resolution infrared radiance data. Part I: Methodology and synthetic cirrus. *To be submitted to the* Journal of Climate.

Kahn, B.H., A. Eldering, M. Ghil, A. Braverman, E.J. Fetzer, and H.M. Steele, 2003: Principal component and sensitivity analysis of cirrus clouds using high-resolution infrared radiance data. Part II: Application to case studies of Atmospheric Infrared Sounder data. *To be submitted to the* Journal of Climate.

Mishchenko, M.I., and L.D. Travis, Capabilities and limitations of a current Fortran implementation of the *T*-matrix method for randomly oriented, rotationally symmetric scatterers, *J. Quant. Spec. Rad. Trans.*, **60**, 309-324, 1998.

Moncet, J.L., and S.A. Clough, 1997: Accelerated monochromatic radiative transfer for scattering atmospheres: Application of a new model to spectral radiance observations. *J. Geophys. Res.*, **102**, 21 853-21 866.